J Nanostruct Chem (2017) 7:207–215
DOI 10.1007/s40097-017-0231-8

ORIGINAL RESEARCH

# Chemisorption of $BH_3$ and $BF_3$ on aluminum nitride nanocluster: quantum-chemical investigations

**Ali Shokuhi Rad**[1]

Received: 7 April 2017 / Accepted: 19 June 2017 / Published online: 26 June 2017


**Abstract** In this study, two functionals (B3LYP and ωB97XD) were used for density functional theory (DFT) calculation of two major boron compounds ($BH_3$ and $BF_3$) adsorption on fullerene-like $Al_{12}N_{12}$ nanocluster. High values of adsorption energy, −268.6 (−244.7) for $BF_3$ and −224.5 (−196.4) kJ/mol for $BH_3$ were found using ωB97XD (B3LYP) functional, indicating strong chemisorption which is the result of Lewis acid–base interaction of adsorbent and adsorbates. The high negative values of ΔG (Gibbs free energy) and ΔH (enthalpy) confirm spontaneous exothermic adsorption process. Further studies were done by taking into account the charge analysis, FMO (frontier molecular orbitals), MEP (molecular electrostatic potential), density of states (DOS), and reactivity of resulted systems.

**Keywords** Fullerene-like cluster · $Al_{12}N_{12}$ Nanocage · Chemisorption · Boron trifluoride · Borane

## Introduction

Borane (trihydridoboron) and boron trifluoride are two inorganic compounds with chemical formulas of $BH_3$ and $BF_3$, respectively. They are drab gases that are famous as substantial reagents in reaction pathway [1, 2]. In addition, they are known as significant Lewis acids (because of the electron deficiency of boron atom in their compounds) and general construction blocks for further boron complexes. Studying the interface conception of different B–N bonds is vital for energy storage viewpoint. Group III-nitrogen compounds are well-recognized as storage energy owing to their lightweight and inherent high releasing energy [3].

Although $BH_3$ itself has not normally used as a reactant; however, it is a potential intermediate in adsorption of diborane, $B_2H_6$, that is broadly used as a source of boron [4]. Similarly, boron halides, including $BF_3$ and $BCl_3$, have been used as substitute probe molecules owing to the $2p^1$ electronic structure of boron that provides a powerful Lewis acid when shared with a halogen atom [5, 6]. The boron atom of $BF_3$ has an unfilled $p^z$-like orbital in perpendicular to the molecular plane and has a propensity to receive electron pairs, and this property causes adsorption of boron compounds. For example in our recent study [7], we investigated the adsorption of some boron compounds on the surface of nitrogen-doped graphene. We found formation of new bond between nucleophilic atom (N) and electrophilic atom (B), whereas there was weak physisorption in the case of pristine graphene. There are various investigations on $BF_3$ and $BH_3$ in literature in this regard. For example, Xu et al. [8] used DFT to study the hydroboration of the Ge(1 0 0)−2 × 1 surface with $BH_3$. Based on their result, the Ge(1 0 0) surface displays rather different surface reactivity to dissociative adsorption of $BH_3$ in comparison with the C(1 0 0) and Si(1 0 0) surfaces. In another work, dissociative adsorption of $BH_3$ on the Si(100) surface has been searched with nonlocal DFT by Konecny and Doren [4]. They revealed that a Si–B bond is constructed through a nucleophilic attack on boron, leaving $BH_2$ and H fragments bonded to the surface.

Abee and Cox [5] searched on $BF_3$ as a probe molecule to interrogate the basicity of $Cr_2O_3$ $(10\bar{1}2)$ surfaces.

After a successful development of CNT and fullerene C60, various spherical fullerene-like configurations

✉ Ali Shokuhi Rad
a.shokuhi@gmail.com; a.shokuhi@qaemiau.ac.ir

[1] Department of Chemical Engineering, Qaemshahr Branch, Islamic Azad University, Qaemshahr, Iran

composed of inorganic non-carbon materials have been stimulated a great deal of interest [9–20]. Strout et al. revealed that the fullerene-like nano-cages $X_{12}Y_{12}$ are the most stable structures among all $(XY)_n$ ($X$ = B, Al, Ga,… and $Y$ = N, P, As, …) semiconductors [9]. $Al_{12}N_{12}$, $Al_{12}P_{12}$, $B_{12}N_{12}$, and $B_{12}P_{12}$ are of great significance because of their high steadiness, large energy band gap, and outstanding chemical and physical properties. Among them, $B_{12}N_{12}$ nanoclusters were synthesized by Oku et al. in 2004 [10]. Different applications of nanostructure materials have been studied in recent literature [11–24]. Because of important roles of boron compounds in different areas of study, recently we rummaged on the chemisorption property of boron trichloride ($BCl_3$) on the surface of $Al_{12}N_{12}$ nanocluster [6]. Following successful potential of mentioned nanocluster as an ideal adsorbent, we persuaded to search on the adsorption of other boron compounds on this kind of nanocluster. As we found, there is no investigation in literature on the $BH_3$ and $BF_3$ adsorption on the $Al_{12}N_{12}$ nanocluster. In this paper, I have employed DFT method to investigate the adsorption of above-mentioned molecules on the surface of $Al_{12}N_{12}$ nanocluster. The attained results were analyzed by considering adsorption energies, the natural bond orbital (NBO) charge transfer, frontier molecular orbitals, density of states, and global indices of activities.

## Computational details

The geometries of $Al_{12}N_{12}$ nanocluster and corresponding boron complexes were fully relaxed at the B3LYP (and ωB97XD)/6−31G** level of theory as implemented in Gaussian 09 suite of program [25]. The suitability of B3LYP functional for different nanostructures has been proved [26–29]. To consider the effect of dispersion on adsorption energies, all relaxed structures were subjected to new optimization using meta-hybrid functional (wB97XD) [30]. For each calculation, the global charge of system was neutral. Frequency calculations have been performed to ensure the stability of the interaction. Adsorption energy ($E_{ad}$) of $BX_3$ ($X$ = F, H) on $Al_{12}N_{12}$ nanocluster is defined as

$$E_b = E_{A112N12-BX3} - (E_{A112N12} + E_{BX3}), \quad (1)$$

where $E_{Al12N12\text{-}BX3}$ is the total energy of the adsorbed $BX_3$ molecule on the surface of nanocluster ($Al_{12}N_{12-}$), and $E_{Al12N12}$ and $E_{BX3}$ are the total energies of the free $Al_{12}N_{12}$ and a free $BX_3$ molecule, respectively.

Natural bond orbital (NBO) analysis [31] is used to follow charge distribution and charge transfer between $BX_3$ and $Al_{12}N_{12}$. Frontier molecular description has been studied to follow the variation in the structure of nanocluster when $BX_3$ is adsorbed. Parr et al. [32] stated the electrophilicity concept. Chemical potential ($\mu$) is defined based on the following eq. [33]:

$$\mu = -(E_{HOMO} + E_{LUMO})/2, \quad (2)$$

where $E_{HOMO}$ is the energy of HOMO and $E_{LUMO}$ is the energy of LUMO. In addition, hardness (ŋ) can be calculated using the Koopmans' theorem [33] as:

$$\eta = (E_{HOMO} + E_{LUMO})/2 \quad (3)$$

Softness ($S$) [33] and electrophilicity ($\omega$) [33] are defined as the following eqs. correspondingly.

$$S = 1/(2\eta) \quad (4)$$

$$\omega = \mu^2/2\eta. \quad (5)$$

## Results and discussion

The electronic structure of $Al_{12}N_{12}$ nanocluster is pretty discussed in different investigations [11–14], so, a comprehensive explanation is not provided here. As shown in Fig. 1, this kind of nanocluster is performed of some tetragon (four membered) and hexagon (six membered) rings. Actually, there are two kinds of Al…N bond through the cluster, one is shared between two hexagon rings (b@66) and another is shared between a hexagon ring and a tetragon ring (b@64). The bond distances are calculated to be 1.79 and 1.86 Å for b@66 and b@64, respectively. The NBO charge allocation in $Al_{12}N_{12}$ nanocluster is also depicted in Fig. 1 (right). It is obvious from Fig. 1 that the charge is uniformly distributed through the nanocluster. Each Al atom has a positive charge of +1.84 e, whereas each N atom has a negative charge of −1.84 e through the structure. As a result, positive and negative sites of cluster correspond to nucleophilic and electrophilic attacks of adsorbates, respectively.

To study the interaction of $BF_3$ and $BH_3$ onto $Al_{12}N_{12}$ nanocluster, firstly I placed the $BX_3$ ($X$ = F, H) molecule at different orientations above the cluster, 1-the B atom of $BX_3$ above the N of cluster, 2-the X atom of $BX_3$ above the N of cluster so that X–B bond has perpendicular orientation than the surface. All these initial configurations were used to fully optimization using two before-mentioned functionals. Despite there are different initial configurations, I found that there is only one relaxed structure (output) for $BF_3$ as well as $BH_3$ upon optimization. Figure 2 depicts side and tope views of adsorbed $BF_3$ and $BH_3$ onto nanocluster. As shown in Fig. 2, adsorption of $BF_3$ and $BH_3$ correspond to the formation of new bond between N of cluster and B of adsorbate. The B…N bond length is 1.45 and 1.59 Å for $Al_{12}N_{12}$–$BF_3$ and $Al_{12}N_{12}$–$BH_3$ complexes,

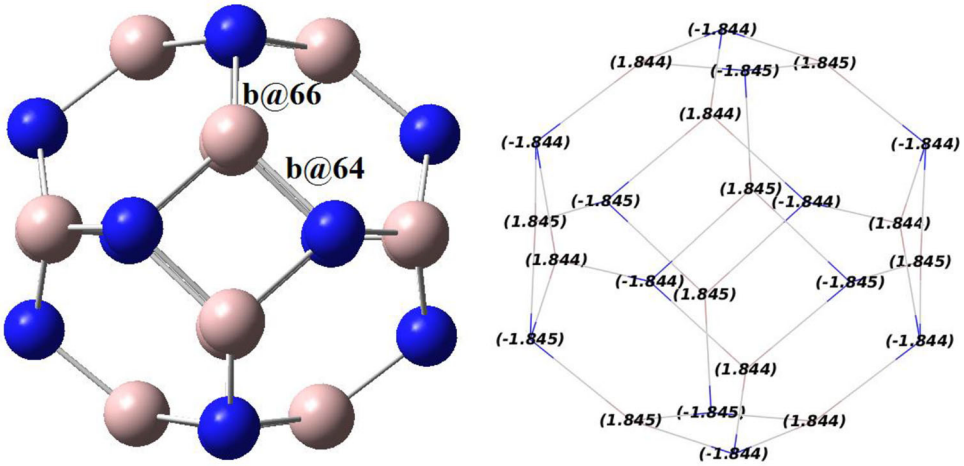


**Fig. 1** Relaxed structure of $Al_{12}N_{12}$ nanocluster along with the NBO charge distribution of nanocluster

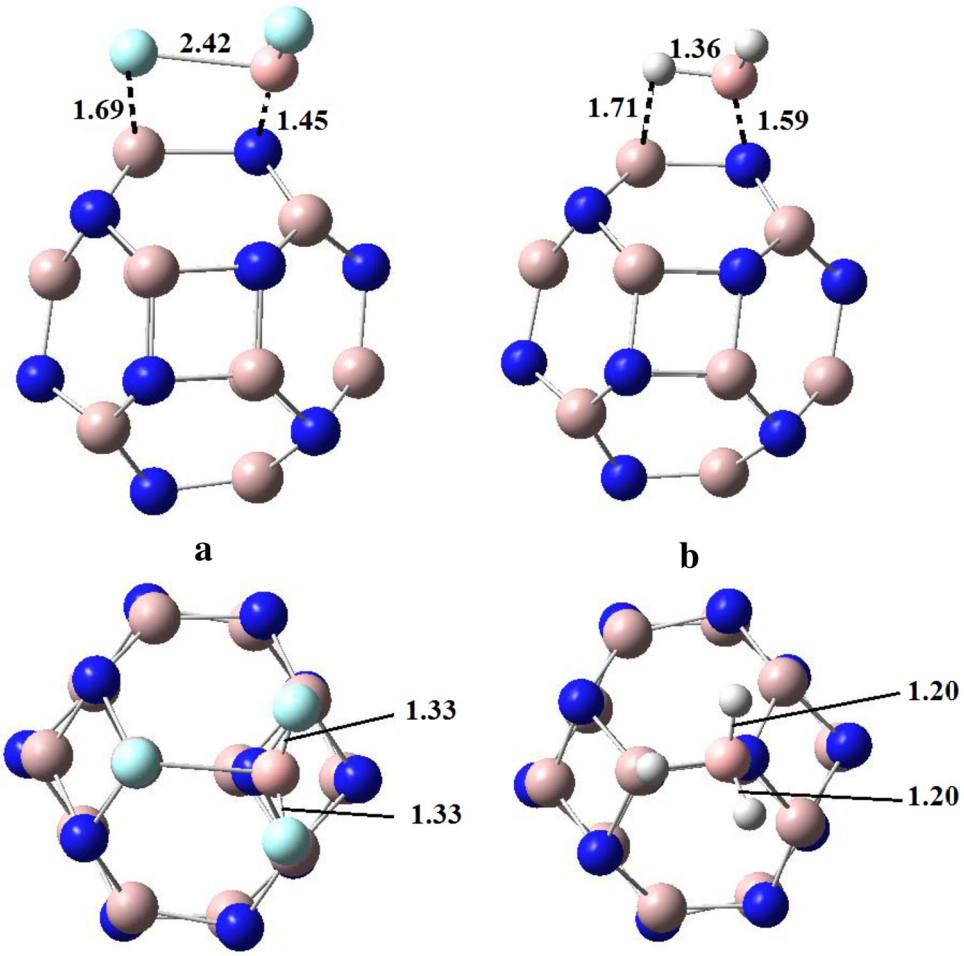


**Fig. 2** Side and top views of adsorbed $BF_3$ and $BH_3$ on $Al_{12}N_{12}$ nanocluster

respectively. The lower distance in the earlier complex more likely relates to the more positively charged boron in $BF_3$ owing to strong electron affinity of F atoms. As a result, more positively charged boron atom in $BF_3$ corresponds to stronger Lewis acid–base interaction. This bond formation results the transferring in hybridizing of B atom from $sp^2$ to $sp^3$. Moreover, we can see another bond formation between the F atom of $BF_3$ and also the H atom of $BH_3$ with the Al atom of nanocluster (both F and H are negatively charged in their related complex). These new

**Table 1** The values of adsorption energy ($E_{ad}$, kJ/mole) using two functionals (wB97XD and B3LYP), nearest equilibrium distance of analyte- surface ($d_e$, Å), mean of bond distances b@66, and b@64 (Å) at the area of interaction, NBO net charge transfer ($Q_{NBO}$, e), change in the enthalpy and Gibbs free energy (kJ/mol)

| System | $E_{ad}$ (wB97XD) | $E_{ad}$ (B3LYP) | $d_e$ | b@66 | b@64 | $Q_{NBO}$ | ΔH | ΔG |
|---|---|---|---|---|---|---|---|---|
| $Al_{12}N_{12}$ | – | – | – | 1.79 | 1.86 | – | – | – |
| $Al_{12}N_{12}$–$BF_3$ | −268.6 | −244.7 | 1.45 | 2.03 | 1.92 | −0.247 | −240.3 | −195.1 |
| $Al_{12}N_{12}$–$BH_3$ | −224.5 | −196.4 | 1.59 | 1.92 | 1.87 | −0.241 | −187.3 | −140.6 |

bonds formation is because of transferring the density of electron from F and H atoms (which are rich in electron) to unoccupied orbital of Al atom of nanocluster. It is obvious that the bond length of Al…F and Al…H are calculated to be 1.69 and 1.71 Å, respectively, which are comparable with B…N bond in their complexes.

The experimental bond length of B–H and B–F in free $BH_3$ and $BF_3$ molecules is reported 1.19 and 1.31 Å, respectively [5, 34], which are very close to the values of 1.194 and 1.317 Å calculated by this study. It is shown in Fig. 2 that after adsorption of $BF_3$ molecule, fully dissociation in one of the B-F bonds is happened, whereas partial dissociation in one of the B–H bonds is resulted. In the case of $BF_3$, one B…F bond is elongated to 2.42 Å (83.3% increase) and two other bonds are partially extended to 1.33 Å. So, because of the large change in one of the bonds in the molecule, we can conclude fully dissociation of $BF_3$ upon adsorption on $Al_{12}N_{12}$ nanocluster. On the other hand, for $BH_3$, the elongation is less pronounced. It is shown in Fig. 2 that one of the bond lengths of B…H reaches to 1.36 Å (13.3% increase) and two other reach to 1.20 Å upon adsorption which attribute to the partial dissociation of molecule.

The values of adsorption energy are listed in Table 1. We can see that the adsorption of $BF_3$ and $BH_3$ on the surface of $Al_{12}N_{12}$ nanocluster corresponds to releasing energy of −244.7 and −196.4 kJ/mol (based on B3LYP functional), and −268.6 and −224.5 kJ/mol (based on ωB97XD functional), respectively. The difference between the values of adsorption energy achieved by two functionals reveals that the dispersion parameter plays an important role in interaction. All of these values of adsorption are categorized in chemisorption region. In addition, considerable difference between the results of two functionals suggests that dispersion has important role in adsorption process of this study. The results of adsorption energies are totally in agreement with the results of bond distances, the higher adsorption energy corresponds to the lower bond distance. Moreover, calculated value of adsorption energy are greatly higher than what reported for $BH_3$ adsorption on Si(100) surface (≃180 kJ/mole, [4]), and $BF_3$ adsorption on α-$Cr_2O_3$ $(10\overline{1}2)$ (≃133 kJ/mole, [5]).

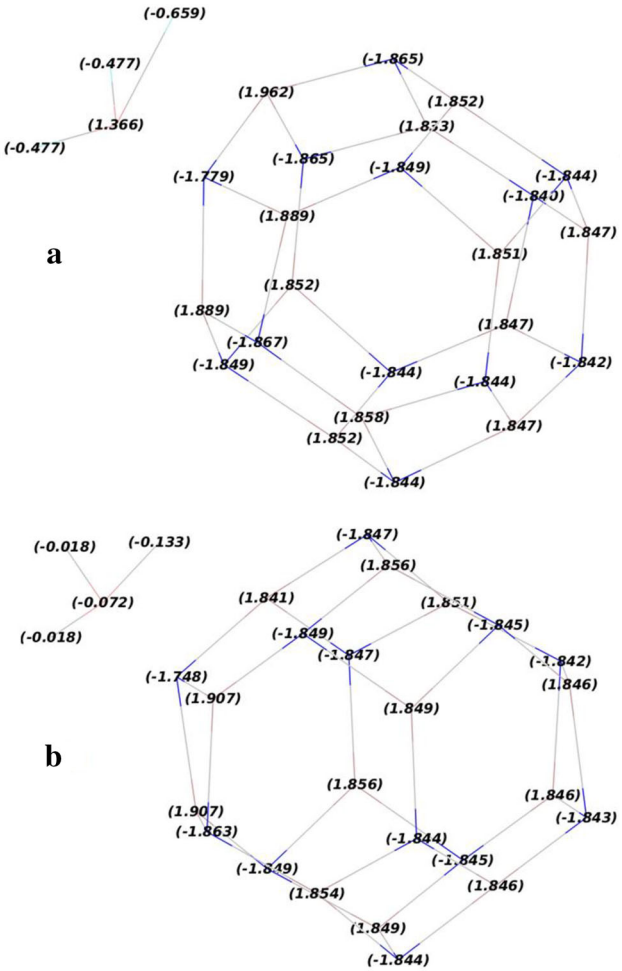


**Fig. 3** The NBO charge allocations after $BF_3$ (**a**), and $BH_3$ (**b**) adsorption

Despite the high changes in the electronic structure of adsorbates, the changes in the electronic structure of nanocluster are also important. It is shown in Table 1 that the Al…N bonds in b@66 (b@64) are changed from 1.79 (1.86) Å for pristine nanocluster to 2.03 (1.92) for $BF_3$ and 1.92 (1.87) for $BH_3$ adsorbed systems. It is obvious that the effect of $BF_3$ adsorption on the electronic structure of nanocluster is more pronounced compared to $BH_3$ which is attributed to the stronger interaction in the earlier complex. By adsorption of $BF_3$ and $BH_3$, not only the bond lengths through the nanocluster are changed, but also the charge

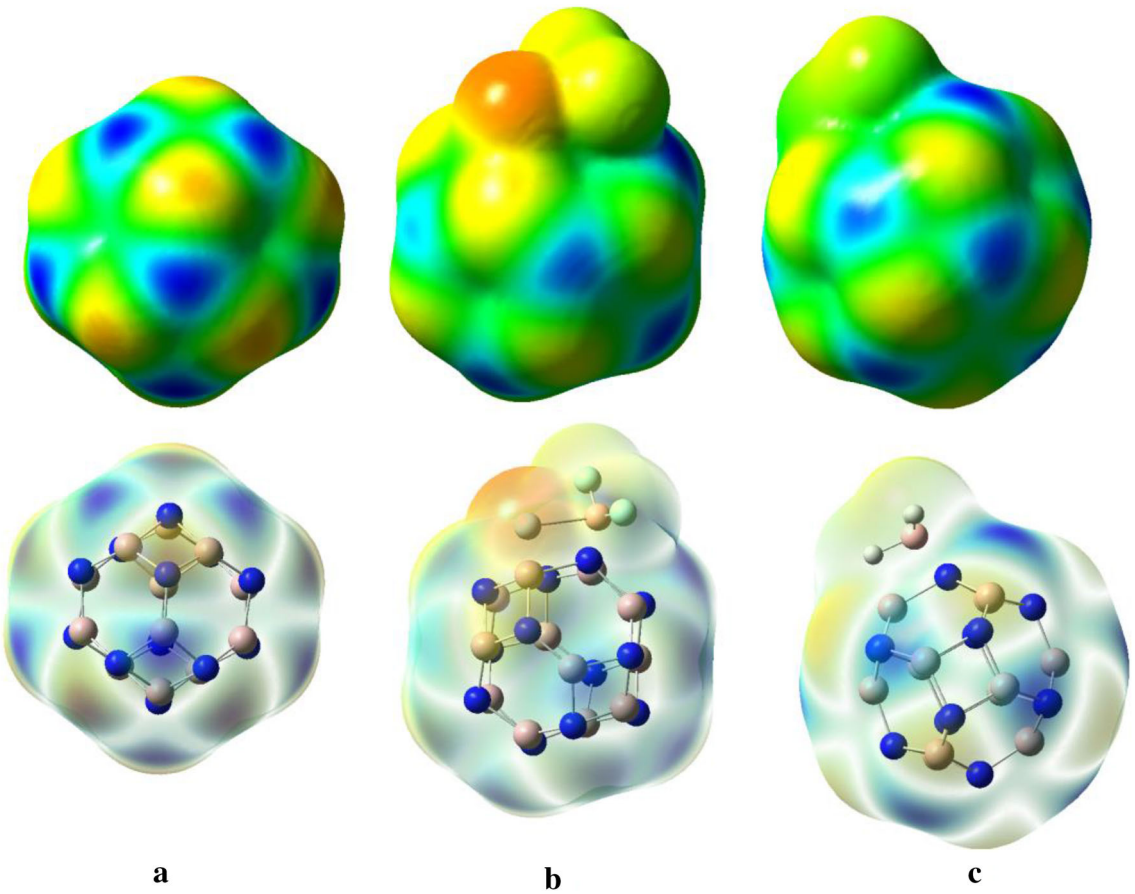


**Fig. 4** The MEP of pristine $Al_{12}N_{12}$ nanocluster (**a**) along with its complexes with $BF_3$ (**b**) and $BH_3$ (**c**)

allocation on each atom significantly is effected (see Fig. 3). By comparing the NBO charge distribution of pristine nanocluster (Fig. 1, right) with that of complexes (Fig. 3), one can conclude significant change especially in the area of interaction, which is considerable in the case of $BF_3$ compared to $BH_3$ adsorption. Along with the stronger interaction of N (of nanocluster) with boron atom of $BF_3$ rather than $BH_3$, the higher change in the electronic structure of nanocluster upon adsorption of BF3 is also effected by the stronger Lewis acid–base interaction between F atom (of $BF_3$) and Al atom (of nanocluster) compared to that interaction between the same Al atom and H atom (of $BH_3$). Therefore, the difference in the NBO charge distribution of two complexes is a result of two different kinds of interaction between corresponding atoms. The values of net charge transfer are also listed in Table 1. As expected, direction of charge transfer is from nanocluster to adsorbates, confirming transfer of charge from nucleophilic atom (N) to electrophilic atom (B). On the other hand, more charge transfer for $BF_3$ adsorption is in accordance to its higher interaction. However, direction of net charge transfer are the resultant of two revers charge transfer; one from N (of cluster) to B, and another from F (H) of adsorbate to Al (of cluster), but the value of the earlier is much higher as expected, resulting overall direction of charge transfer from $Al_{12}N_{12}$ nanocluster to adsorbates.

In order to examine the thermodynamic feasibility of $BF_3$ and $BH_3$ adsorption on the $Al_{12}N_{12}$ at ambient temperature and pressure ($T = 298.14$ K, and $P = 1$ atm), I have calculated free energies ($\Delta G$) and enthalpy changes ($\Delta H$) of each system using the results of vibrational frequency calculations,. The computed values of $\Delta H$ are $-240.3$ and $-187.3$ kJ/mol, and those of $\Delta G$ are $-195.1$ and $-140.6$ kJ/mol, respectively. However, the lower value of $\Delta G$ compared to that of $\Delta H$ is because of the entropic influence. The negative value of Gibbs free energy as well as enthalpy of each system confirms that adsorption of above-mentioned adsorbates is a spontaneous exothermic process.

To better understand the binding sites, I have calculated the molecular electrostatic potentials (MEP) of each system. For this determination, MEP of $Al_{12}N_{12}$ nanocluster and its complexes ($Al_{12}N_{12}$–$BF_3$ and $Al_{12}N_{12}$–$BH_3$) were compared and are given in Fig. 4. For pristine $Al_{12}N_{12}$ nanocluster, Aluminum has positive charge (blue color)

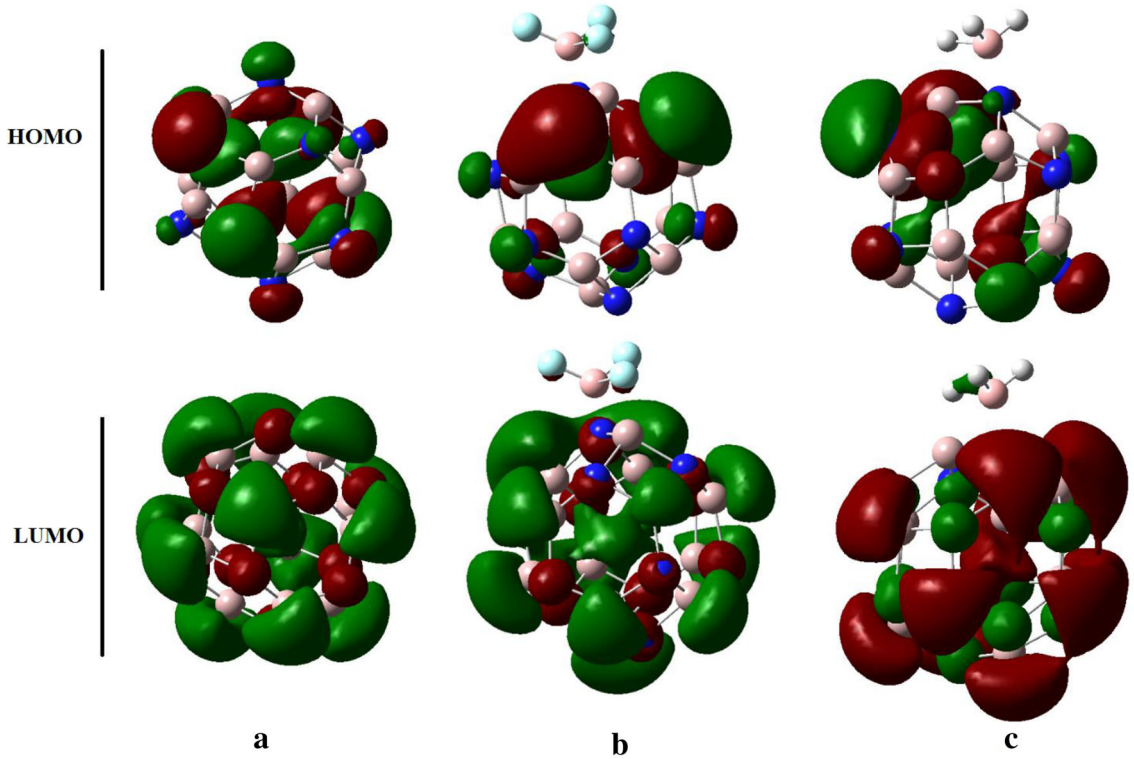


**Fig. 5** HOMO and LUMO distributions of pristine $Al_{12}N_{12}$ (**a**) $Al_{12}N_{12}$–$BF_3$ (**b**), and $Al_{12}N_{12}$–$BH_3$

**Table 2** The electronic properties of free $Al_{12}N_{12}$ and its complexes

| System | $E_{HOMO}$ | $E_{LUMO}$ | $E_g$ | $\eta$ | $\mu$ | $S$ | $\omega$ |
|---|---|---|---|---|---|---|---|
| free $Al_{12}N_{12}$ | −6.472 | −2.541 | 3.931 | 1.965 | −4.506 | 0.254 | 5.157 |
| $Al_{12}N_{12}$–$BF_3$ | −6.380 | −2.762 | 3.618 | 1.809 | −4.571 | 0.276 | 5.767 |
| $Al_{12}N_{12}$–$BF_3$ | −6.474 | −2.605 | 3.869 | 1.934 | −4.539 | 0.258 | 5.315 |

$[Eg = (E_{HUMO} - E_{LUMO})]/ E_{LUMO})]eV.eV$, $[\eta = -(E_{HUMO} - E_{LUMO})/ E_{LUMO})2.2]/eV$, $[\mu = (E_{HOMO} + E_{LUMO})/2]/E_{LUMO})/2]eV.eV$, $S = [1/2\eta]eV^{-1}$, $\omega = [\mu^2/2\eta]$

while the nitrogen has negative charge. The negative charge on N in the nanocluster is not much pronounced (yellow color). After adsorption of $BF_3$ and $BH_3$ molecules, we can see important changes in the blueish and yellowish part of cluster, especially at the area of interaction. The red part of $Al_{12}N_{12}$–$BF_3$ complex attributes to the electronegative F atom of $BF_3$ while no red part can be seen in $Al_{12}N_{12}$–$BH_3$ complex. This is another proving for happening two strong Lewis acid–base interactions (N…B and Al… F) during the earlier complex formation.

Frontier molecular orbitals are also studied to search the effect of $BF_3$ and $BH_3$ adsorption on the electronic properties of $Al_{12}N_{12}$ nanocluster. The outlooks of HOMOs and LUMOs are shown in Fig. 5 and their values are given in Table 2. The spreading of densities also delivers important information concerning the adsorbent capability of $Al_{12}N_{12}$ nanocluster for $BF_3$ and $BH_3$ molecules. As shown in Fig. 5, the HOMO in $Al_{12}N_{12}$ nanocluster is confined on nitrogen atoms, while the LUMO has density homogeneously circulated on the whole nanocluster. Upon $BF_3$ and $BH_3$ adsorption, the densities are redistributed confirming important alterations in the electronic structure of $Al_{12}N_{12}$ nanocluster.

The HOMO–LUMO energies of $Al_{12}N_{12}$ nanocluster are −6.472 and −2.541 eV, correspondingly. As shown in Fig. 5 and the data of Table 2, the adsorption of $BF_3$ and $BH_3$ causes some changes in the electronic structure of the $Al_{12}N_{12}$ nanocluster. While the energy gap of pristine $Al_{12}N_{12}$ nanocluster is 3.931 eV, upon $BF_3$ and $BH_3$ adsorption, the energy gaps are reduced to 3.618 and 3.869 eV, respectively.

For $BF_3$ adsorption, the HOMO of resulted system increases while the LUMO decreases; however, the change in the LUMO is more pronounced than HOMO, resulting in

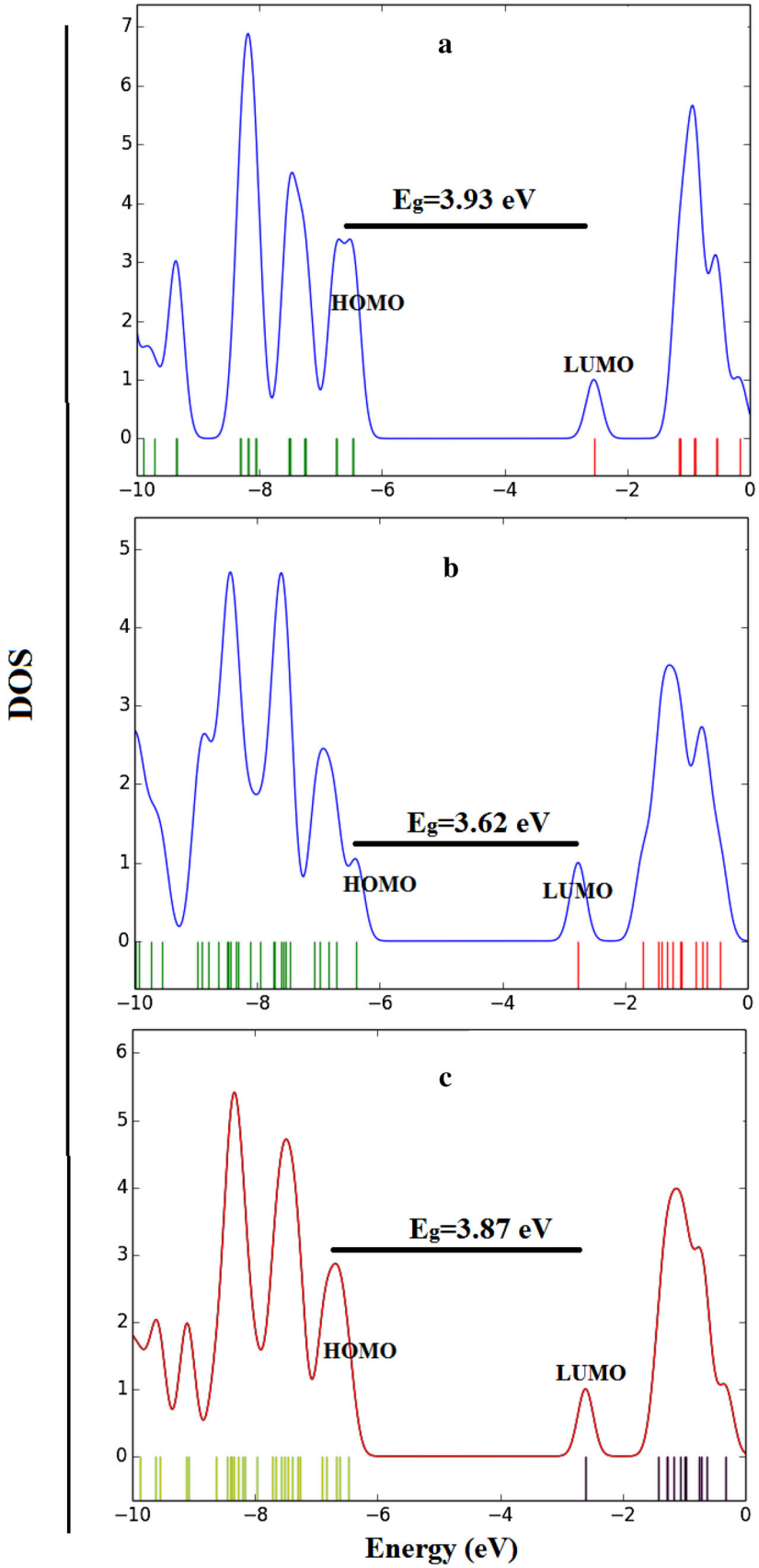


**Fig. 6** Density of states of pristine $Al_{12}N_{12}$ (a) $Al_{12}N_{12}$–$BF_3$ (b), and $Al_{12}N_{12}$–$BH_3$

a decrease in the energy gap of system. On the other hand, upon adsorption of $BH_3$, the energy of HOMO approximately remains unchanged while the LUMO decreases, resulting in a little decrease in the energy gap of system.

Density of states (DOS) of pristine $Al_{12}N_{12}$ and $Al_{12}N_{12}$–$BF_3$ and $Al_{12}N_{12}$–$BH_3$ complexes is studied in order to obtain more understanding the effect of adsorption (See Fig. 6). Some new energy states appear upon adsorption of both $BF_3$ and $BH_3$ molecules. These new states appear near the frontier molecular orbitals, which confirm case of strong hybridizing. The alteration in electronic properties is very essential for the development of sensors. Alteration in HOMO–LUMO causes change in electrical conductivity, which is the prime factor in the design of electrochemical sensors. Association between conductivity and $E_g$ can was determined as Eq. (6) [35].

$$\sigma\alpha \exp\left(-E_g/kT\right), \tag{6}$$

where it could be understood that a small lessening in $E_g$ leads to meaningfully greater electrical conductivities.

The global indices of reactivity for pristine $Al_{12}N_{12}$ and its complexes are given in Table 2. They are pretty vital parameters owing to they exemplify the reactivity and steadiness of a system. Entertainingly, the hardness of nanocluster (1.965 eV) decreases on complexation with $BF_3$ (1.809 eV) and $BH_3$ (1.934 eV). One can see that the change in hardness is comparatively small for $BH_3$ adsorption ($\Delta\eta = -0.031$ eV) whereas meaningfully large alteration is observed for $BF_3$ adsorption ($\Delta\eta = -0.156$). Meanwhile, hardness attributes to the steadiness of a complex toward distortion in the attendance of electrical field, based on the result, the $Al_{12}N_{12}$ complexes are more susceptible to deformation under electrical field than pristine nanocluster. Softness inversely changes compared to hardness, hence, it is predictable that softness for $Al_{12}N_{12}-BF_3$ and $Al_{12}N_{12}-BH_3$ will increase, resulting increase in the reactivity of complexes.

## Conclusion

$BF_3$ and $BH_3$ with a low-lying empty orbital are strong Lewis acids, so their capability to accept electrons along with their planar geometries suggests that nucleophilic attack by a nucleophilic atom is performed. The goal of this research is investigation on the adsorption properties of $BF_3$ and $BH_3$ molecules on $Al_{12}N_{12}$ nanocluster considering DFT method. I found fully dissociative adsorption for $BF_3$ and partial dissociative adsorption for $BH_3$ molecules. The computed values of $\Delta H$ are $-240.3$ and $-187.3$ kJ/mol, and those of $\Delta G$ are $-195.1$ and $-140.6$ kJ/mol, for $BF_3$ and $BH_3$ adsorption, respectively. The negative value of Gibbs free energy approves that adsorption of above-mentioned adsorbates is a spontaneous process. Results of frontier molecular orbitals confirm some important changes in the electronic structure of the nanocluster upon adsorption.

**Acknowledgements** I highly acknowledge the financial support received from the Iran Nanotechnology Initiative Council, Iran.



## References

1. Rasul, G., Prakash, S.G.K., Olah, G.A.: Complexes of CO2, COS, and CS2 with the super Lewis Acid BH4+ contrasted with extremely weak complexations with BH3: theoretical calculations and experimental relevance. J. Am. Chem. Soc. **121**, 7401–7404 (1999)
2. Brinck, T., Murray, J.S., Politzer, P.: A Computational analysis of the bonding in boron trifluoride and boron trichloride and their complexes with ammonia". Inorg. Chem. **32**, 2622–2625 (1993)
3. Leskiw, B.D., Castleman Jr., A.W., Ashman, C., Khanna, S.N.: Reactivity and electronic structure of aluminum clusters: the aluminum–nitrogen system. J. Chem. Phys. **114**, 1165–1169 (2001)
4. Konecny, R., Doren, D.J.: Adsorption of $BH_3$ on Si (100)−(2×1). J. Phys. Chem. B **101**, 10983–10985 (1997)
5. Abee, M.W., Cox, D.F.: BF3 Adsorption on α-$Cr_2O_3$ ($10\overline{1}2$): Probing the Lewis basicity of surface oxygen anions. J. Phys. Chem. B **105**, 8375–8380 (2001)
6. Rad, A.S., Ayub, K.: DFT study of boron trichloride adsorption on the surface of Al12N12 nanocluster. Mol. Phys. **115**, 879–884 (2017)
7. Rad, A.S., Shadravan, A., Soleymani, A.A., Motaghedi, N.: Lewis acid-base surface interaction of some boron compounds with N-doped graphene, first principles study. Curr. Appl. Phys. **15**, 1271–1277 (2015)
8. Xu, Y.J., Li, J.Q.: The dissociative adsorption of borane on the Ge (100)–2×1 surface: a density functional theory study. Appl. Surf. Sci. **252**, 5855–5860 (2006)
9. Strout, D.L.: Structure and stability of boron nitrides: isomers of $B_{12}N_{12}$. J. Phys. Chem. A **104**, 3364–3366 (2000)
10. Oku, T., Nishiwaki, A., Narita, I.: Formation and atomic structure of $B_{12}N_{12}$ nano-cage clusters studied by mass spectrometry and cluster calculation. Sci. Tech. Adv. Mater. **5**, 635–638 (2004)
11. Rad, A.S., Ayub, K.: A comparative density functional theory study of guanine chemisorption on $Al_{12}N_{12}$, $Al_{12}P_{12}$, $B_{12}N_{12}$, and $B_{12}P_{12}$ nano-cages. J. Alloys Compd. **672**, 161–169 (2016)
12. Rad, A.S., Ayub, K.: Adsorption of pyrrole on $Al_{12}N_{12}$, $Al_{12}P_{12}$, $B_{12}N_{12}$, and $B_{12}P_{12}$ fullerene-like nano-cages, a first principles study. Vacuum **131**, 135–141 (2016)
13. Rad, A.S.: Study on the surface interaction of Furan with $X_{12}Y_{12}$ (X = B, Al, and Y = N, P) semiconductors: DFT calculations. Heteroat. Chem. **27**, 316–322 (2016)
14. Ayub, K.: Are phosphide nano-cages better than nitride nano-cages? A kinetic, thermodynamic and non-linear optical properties study of alkali metal encapsulated X12Y12 nano-cages. J. Mater. Chem. C **4**, 10919–10934 (2016)

15. Wang, Q., Sun, Q., Jena, P., Kawazoe, Y.: Potential of AlN nanostructures as hydrogen storage materials. ACS Nano **3**, 621–626 (2009)
16. Rad, A.S., Ayub, K.: Ni adsorption on $Al_{12}P_{12}$ nano-cage: a DFT study. J. Alloys Compd. **678**, 317–324 (2016)
17. Rad, A.S., Ayub, K.: Detailed surface study of adsorbed nickel on $Al_{12}N_{12}$ nano-cage. Thin Solid Films **612**, 179–185 (2016)
18. Rad, A.S., Ayub, K.: Enhancement in hydrogen molecule adsorption on $B_{12}N_{12}$ nano-cluster by decoration of nickel. Int. J. Hydrogen Energy **41**, 22182–22191 (2016)
19. Rad, A.S., Ayub, K.: Coordination of nickel atoms with $Al_{12}X_{12}$ (X = N, P) nano-cages enhances $H_2$ adsorption: a surface study by DFT. Vacuum **133**, 70–80 (2016)
20. Iqbal, J., Ayub, K.: Theoretical study of the non linear optical properties of alkali metal (Li, Na, K) doped aluminum nitride nanocages. RSC Advances **687**, 94228–94235 (2016)
21. Rad, A.S., Ayub, K.: Adsorption properties of acetylene and ethylene molecules onto pristine and Nickel-decorated $Al_{12}N_{12}$ nanoclusters. Mat. Chem. Phys **194**, 337–344 (2017)
22. Rad, A.S., Ayub, K.: Adsorption of thiophene on the surfaces of X12Y12 (X = Al, B, and Y = N, P) nanoclusters; A DFT study. J. Mol. Liq. **238**, 303–309 (2017)
23. Rad, A.S., Ayub, K.: $O_3$ and $SO_2$ sensing concept on extended surface of $B_{12}N_{12}$ nanocages modified by Nickel decoration: a comprehensive DFT study. Solid State Sci. **69**, 22–30 (2017)
24. Rad, A.S., Zareyee, D.: Adsorption properties of $SO_2$ and $O_3$ molecules on Pt-decorated graphene: a theoretical study. Vacuum **130**, 113–118 (2016)
25. Frisch, M. J.: Gaussian 09, Revision E.01, Wallingford CT (2009)
26. Chen, L., Xu, C., Zhang, X.-F., Zhou, T.: Raman and infrared-active modes in MgO nanotubes. Physica E **41**, 852–855 (2009)
27. Rad, A.S.: Study of dimethyl ester interaction on the surface of Ga-doped graphene: Application of density functional theory. J. Mol. Liq. **229**, 1–5 (2017)
28. Rad, A.S., Sani, E., Binaeian, E., Peyravi, M., Jahanshahi, M.: DFT study on the adsorption of diethyl, ethyl methyl, and dimethyl ethers on the surface of gallium doped graphene. Appl. Surf. Sci. **401**, 156–161 (2017)
29. Rad, A.S., Jouibary, Y.M., Foukolaei, V.P., Binaeian, E.: Study on the structure and electronic property of adsorbed guanine on aluminum doped graphene: first principles calculations. Curr. Appl. Phys. **16**, 527–533 (2016)
30. Chai, J.D., Head-Gordon, M.: Long-range corrected hybrid density functionals with damped atom–atom dispersion corrections. Phys. Chem. Chem. Phys. **10**, 6615–6620 (2008)
31. Reed, A.E., Weinstock, R.B., Weinhold, F.: Natural population analysis. J. Chem. Phys. **83**, 735–746 (1985)
32. Parr, R.G., Szentpaly, L., Liu, S.: Electrophilicity Index. J. Am. Chem. Soc. **121**, 1922–1924 (1999)
33. Koopmans, T.: Ordering of wave functions and eigenenergies to the individual electrons of an Atom. Physica **1**, 104–113 (1934)
34. Kawaguchi, K.: Fourier transform infrared spectroscopy of the $BH_3$ $\nu_3$ band". The J. Chem. Phys. **96**, 3411 (1992)
35. Li, S.: Semiconductor Physical Electronics, 2nd edn. Springer, Berlin (2006)